

Autophosphorylation and ADP Regulate the Ca^{2+} -Dependent Interaction of Recoverin with Rhodopsin Kinase[†]

Daulet K. Satpaev,[‡] Ching-Kang Chen,[§] Anthony Scotti,^{||} Melvin I. Simon,[§] James B. Hurley,^{||} and Vladlen Z. Slepak^{*,‡}

Department of Molecular and Cellular Pharmacology, University of Miami School of Medicine, Miami, Florida 33136, Division of Biology, California Institute of Technology, Pasadena, California 91125, and Department of Biochemistry and Howard Hughes Medical Institute, Box 357370, University of Washington, Seattle, Washington 98195

Received March 3, 1998; Revised Manuscript Received April 9, 1998

ABSTRACT: Recoverin is a 23 kDa myristoylated Ca^{2+} -binding protein that inhibits rhodopsin kinase. We have used surface plasmon resonance to investigate the influences of Ca^{2+} , myristoylation, and adenine nucleotides on the recoverin–rhodopsin kinase interaction. Our analyses confirmed that Ca^{2+} is required for recoverin to bind RK. Myristoylation had little effect on the affinity of recoverin for the kinase, but it raised the $K_{0.5}$ for Ca^{2+} from 150 nM for nonacylated recoverin to 400 nM for myristoylated recoverin. Finally, our studies also revealed two separate and previously unreported effects of adenine nucleotides on the recoverin–rhodopsin kinase binding. The interaction is weakened by autophosphorylation of the kinase, and it is strengthened by the presence of ADP.

Phosphorylation of rhodopsin plays an important role in phototransduction by quenching photoactivated rhodopsin (R^*) (1). The enzyme that phosphorylates R^* , rhodopsin kinase (RK), is inhibited by Ca^{2+} in vitro in the presence of recoverin, a 23 kDa calcium-binding protein that is present in rod and cone photoreceptors (2–8).

RK is a member of a family of kinases, GRK's, that phosphorylate G-protein-coupled receptors (9). RK (also known as GRK1) and GRK5 are unique among members of this family in that they undergo autophosphorylation, but the functional consequences of RK autophosphorylation have not yet been understood (10, 11). Reported mutagenesis studies have so far failed to resolve the role of autophosphorylation because the mutations designed to mimic constitutively unphosphorylated or phosphorylated RK both had the same effect of decreasing the specificity of RK for bleached versus unbleached rhodopsin (12).

The amino terminus of recoverin is covalently modified by a myristoyl (14:0) or other short-chain fatty acyl residue (13). This group is solvated in the Ca^{2+} -bound form of the protein, and it can enhance recoverin's interaction with membranes (14–19). Myristoylated and nonmyristoylated forms of recoverin have been produced in *E. coli* in the presence or absence of *N*-myristoyl transferase (20). Fatty acylation is not essential for the ability of recoverin to inhibit RK at saturating Ca^{2+} , but it may enable recoverin to inhibit RK at physiologic levels of Ca^{2+} (7, 18, 21, 22).

Recoverin and RK bind directly in the presence of Ca^{2+} (7, 23). Here, we have used surface plasmon resonance (SPR) to study the kinetics of the recoverin–RK interaction and to examine factors that influence the protein–protein association. SPR measures interactions between macromolecules directly and in real time by monitoring changes in the refractive index that occur as a ligand binds to a surface within a microflow cell (24). Our findings confirm the Ca^{2+} dependence of the recoverin–RK interaction and show that association and dissociation of recoverin and RK occur rapidly. We found that myristoylation has no significant effect on the protein–protein interaction in the absence of phospholipid membranes. Our studies also revealed a previously unrecognized effect of adenine nucleotides upon the recoverin–RK interaction. Autophosphorylation blocks the ability of RK to bind recoverin while ADP enhances the interaction.

MATERIALS AND METHODS

Recoverin was prepared from recombinant *E. coli* (20). RK was isolated from recombinant SF9 cells and purified on an affinity column with immobilized nonmyristoylated recoverin as described previously (7).

Surface Plasmon Resonance Analysis. All the experiments presented in this report were performed on a BIAcore 2000 instrument. Recoverin was immobilized using the basic protocol recommended by manufacturer's manual for coupling of proteins via cysteine groups. The surface of a carboxymethylated dextran-coated sensor chip (CM5 research grade; BIAcore, Inc.) was activated with EDC/NHS (*N*-ethyl-[(*N*′-dimethylamino)propyl]carbodiimide/*N*-hydroxy-succinimide) for 5 min and then modified with PDEA [2-(2-pyridinyldithio)ethanamine hydrochloride] for 5 min. In a typical experiment, recoverin at 0.01 mg/mL in 10 mM acetate buffer, pH 4.5, was injected for 5 min at 5 $\mu\text{L}/\text{min}$. A small fraction of recoverin (<5%) was attached to the

[†] This study was supported in part by grants from the Department of the Navy (96PRO7143-00) and from the American Heart Association Florida Affiliate, Inc. (Initial Investigator Award 9603008) to V.Z.S. and from the National Eye Institute (EY06641) to J.B.H. D.K.S. was supported by the American Heart Association Florida Affiliate, Inc., Postdoctoral Fellowship 9703012.

* Corresponding author.

[‡] University of Miami School of Medicine.

[§] California Institute of Technology.

^{||} University of Washington.

surface noncovalently and was removed by a 1 min pulse of 6 M guanidine hydrochloride. The surface was then treated by a 5 min injection of 1–10 mM cysteine to block the residual reactive groups. In a typical experiment, we immobilized approximately 1000 resonance units (RU) of recoverin (1000 RU is approximately 1 ng/mm²). We have used such high immobilization levels of recoverin in most experiments in order to reliably see the inhibitory effects of reduced Ca²⁺ and ATP on its binding to RK. The amount (surface density) of covalently immobilized recoverin was determined as the difference of the SPR signal between the readings before and after ligand coupling, i.e., following PDEA injection and after the wash by guanidine. In experiments comparing nonacylated (NA) and myristoylated (14:0) forms of recoverin, the amounts of immobilized proteins were carefully monitored during the coupling and, if needed, equalized by additional short injections of protein so that the difference between the levels of immobilized proteins was less than 10%. In a series of preliminary experiments, we have also used coupling of recoverin via amine groups, directly following activation of the CM5-chip by EDC/NHS. The kinetics of binding as well as its sensitivity to Ca²⁺ and adenine nucleotides were very similar to those obtained with cysteine-coupled recoverin. However, the overall binding of RK to NH₂-coupled ligand was 5–10-fold less, apparently due to coupling of recoverin via lysine residues that are necessary for the protein–protein interaction or because of denaturation of recoverin due to the coupling. Since there are 30 lysine residues in a recoverin molecule and only 1 cysteine, the thiol-coupling procedure has apparently resulted in a surface with uniform ligand orientation.

To analyze recoverin–RK interaction, we diluted RK in a running buffer [20 mM Tris, pH 7.5, 100 mM NaCl, 0.1 mM CaCl₂, 1 mM MgCl₂, 0.005% nonionic detergent P20 (BIACORE, Inc.), and 0.01 mg/mL BSA]. The detergent did not have an effect upon the kinetics of the regulation of recoverin–RK interaction, but allowed us (as the introduction of BSA) to reduce the nonspecific binding of RK. This Ca²⁺-independent binding was detected in the absence of detergent and BSA at both recoverin and control (no recoverin) surfaces. For determination of the Ca²⁺ dependence, RK was diluted 20–50-fold in buffers containing defined free Ca²⁺ concentrations. The Ca²⁺ solutions used in Figure 3 were purchased from Molecular Probes, Inc. (Eugene, OR), but we obtained similar results with solutions made from EGTA buffers and Ca²⁺ solutions quantified by atomic absorption (25) and with BAPTA buffers verified by a Ca²⁺-sensitive electrode. Solutions of RK were injected at a flow rate of 5 or 10 μ L/min for the time intervals indicated. Sensograms were analyzed by BIAEvaluation 2.1 software (BIACORE, Inc.). Dissociation rates were estimated assuming single-exponential decay. Dissociation rates for the interactions reported here (~ 0.1 s⁻¹) were near the time resolution limits of the BIAcore detector. These analyses were further complicated by apparent rapid rebinding, a characteristic of proteins with association rates $> 10^5$ M s⁻¹.

Rhodopsin Kinase Autophosphorylation and Dephosphorylation. For autophosphorylation, RK was incubated at room temperature in the presence of ATP in a buffer also containing 20 mM Tris, pH 7.5, 100 mM NaCl, and 1 mM MgCl₂. The concentration of ATP was 0.1 mM unless

specified otherwise. To monitor the reaction, 0.25–0.5 μ Ci of [³²P] γ -ATP (NEN) was added to the reaction, and phosphate incorporation was monitored, following SDS–PAGE, autoradiography, and scintillation counting of the bands as described previously (7). The radioactive labeling coincided with a near-quantitative upward shift of the RK band as revealed by Coomassie staining of the gel and rapidly (< 5 min at room temperature) reached plateau, indicating that phosphorylation was complete within this time frame. For dephosphorylation, phosphorylated RK was mixed with a protein phosphatase for various times at room temperature or at 30 °C. In some experiments, phospho-RK was desalted on a Sephadex minicolumn to remove ATP. We have tested three different protein phosphatases: recombinant protein phosphatase λ (Calbiochem or Sigma), recombinant muscle protein phosphatase 1 (PP1) provided by Dr. E. Lee (University of Miami), and protein phosphatase type 2A (PP2A) isolated from human red cells (Upstate Biotechnology, Inc.). The first two enzymes could dephosphorylate RK only partially (20–40%) when added at high concentrations and upon long incubations. In contrast, PP2A dephosphorylated RK completely and rapidly even in the presence of ATP. For dephosphorylation reaction, 0.2 unit of PP2A was mixed in a 100 μ L assay with 1–3 μ M RK and incubated 2–5 min at room temperature. Dephosphorylation was monitored, following analysis by SDS–PAGE, by radioautography and Coomassie staining. For the analysis of the effect of RK autophosphorylation and dephosphorylation upon RK interaction with recoverin, an aliquot of the reaction mix was injected across the BIAcore sensor chip with immobilized recoverin.

RESULTS

Previous studies showed that recoverin associates directly with RK (7, 23) and inhibits its activity in vitro (2–8). We used SPR to further characterize the recoverin–RK interaction because this method allows quantitative assessment of protein–protein binding parameters. We coupled recoverin via its unique cysteine (Cys39) to a BIAcore chip. This method was chosen because coupling via lysine residues reduced recoverin's ability to bind RK. Figure 1A shows that introducing purified RK to the recoverin-coated surface elicited a rapid SPR response. Several lines of evidence show that this represents a specific interaction between recoverin and RK. First, RK does not bind substantially to a control surface without recoverin. Second, BSA and several other proteins including GRK5, transducin α , transducin $\beta\gamma$, phosducin and, glutathione *S*-transferase do not bind to immobilized recoverin. Third, binding of RK was proportional to the amount of recoverin immobilized on the chip. Finally, we found that the recoverin–RK interaction depends on two types of factors, Ca²⁺ and adenine nucleotides, that specifically interact with recoverin and RK, respectively.

The SPR signal depends on RK concentration and on the amount of recoverin linked to the sensor chip (Figure 1A). The maximum concentrations of RK in our preparations (3 μ M) did not saturate the surface. However, the shape of the binding curve shown in Figure 1B indicates that half-maximal binding occurs at approximately 0.5–1 μ M RK. At concentrations of RK above 3 μ M, we have observed an increase of irreversible Ca²⁺-independent binding perhaps

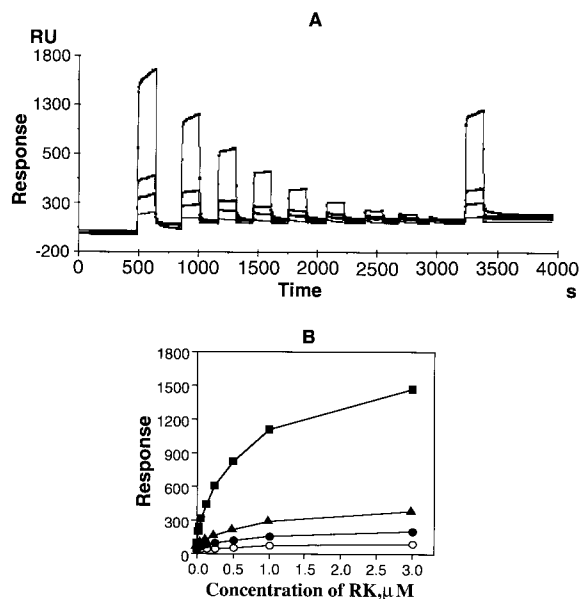


FIGURE 1: Interaction of RK with immobilized recoverin on BIAcore. Recombinant myristoylated recoverin was coupled to the sensor chip as described under Materials and Methods. Surfaces with three densities (1000, 260, and 130 RU) of immobilized ligand were prepared by exposing the activated surfaces in the three channels on the chip to recoverin for various times. As a control, cysteine was immobilized on the fourth channel. A solution of RK was perfused over the four surfaces simultaneously at 10 $\mu\text{L}/\text{min}$ flow rate. Consecutive injections of samples with decreasing RK concentration (3 μM ; 1 μM ; 500 nM, 250, 125, 62, 31, and 15 nM; and buffer alone) were made to determine the dose dependence of the interaction. A second injection of RK at 1 μM was made at the end of the series (approximately 3250 s) to confirm that recoverin was still functional by the end of the experiment. The Ca^{2+} concentration in the running buffer and RK samples was 100 μM (A) Sensograms (raw data) obtained during injections of RK over the four surfaces with different amounts of coupled recoverin; the lowest trace is the change of refractive index on the control surface. (B) Dose dependence of RK binding. Squares, binding to the surface with 1000 RU of recoverin; black triangles, 260 RU; black circles, 130; white circles, control surface (no recoverin, only cysteine is coupled to the surface).

due to precipitation of RK on the surface. The molecular mass of RK (66 kDa) is about 3 times larger than that of recoverin (23 kDa). Since the SPR response is a function of mass accumulated near the sensor surface (24), the increase of the signal detected upon binding of RK in a 1:1 complex should have been 3 times the amount of attached recoverin. In our experiments, however, the saturation was achieved when the amount of bound RK was approximately 1.5 times the amount of recoverin. This ratio was independent of recoverin's surface density, arguing against a possibility of a 2:1 recoverin–RK complex. We thus estimate that only 50% of the immobilized recoverin was competent to bind the kinase. The remainder of the potential binding sites may be recoverin molecules that are denatured or hidden within the dextran matrix on the chip and are inaccessible to the larger RK molecules. The amount of coupled recoverin could also be overestimated because of minor contaminants in the preparation which contributed to the total SPR response after the ligand immobilization. We used RK concentrations from the linear portion of the binding curve, typically 250 nM, in all subsequent experiments.

RK binds rapidly to immobilized recoverin in the presence of 100 μM Ca^{2+} with an association rate constant (k_a) of

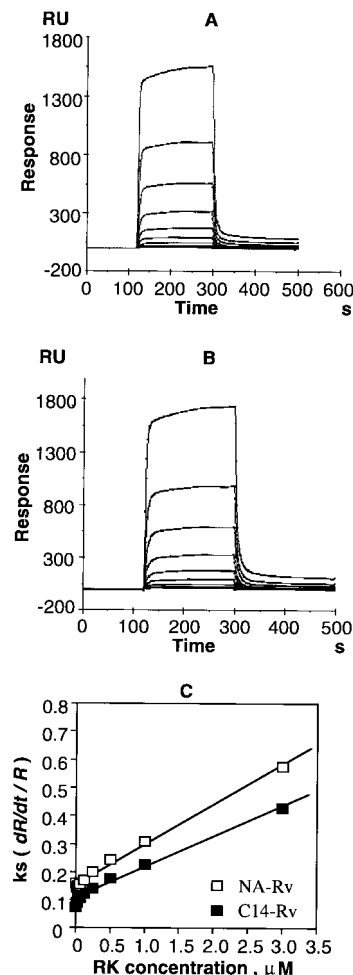


FIGURE 2: Kinetics of RK binding to immobilized nonacylated and myristoylated recoverin. Equal amounts of recombinant nonacylated (NA-Rv) and myristoylated (C14-Rv) recoverin forms were immobilized on the two channels of the sensor chip, and increasing concentrations of RK were injected across at 10 $\mu\text{L}/\text{min}$. (A) Overlay plot of sensograms of consecutive injections over NA-Rv. (B) Overlay plot of consecutive injections over C14-Rv. (C) k_s vs C . Estimation of the binding constants using the plot $k_s = (dR/dt)/R$ (rate of binding versus level of binding) depending on RK concentration. The intercept is k_d ; the slope of the line is k_a .

10^5 M s^{-1} . From the analysis of recoverin–RK complex decay, the dissociation rate constant (k_d) is 0.1 s^{-1} , and the half-life of the complex is less than 5 s. The k_d was also determined from the analysis of association phases of sensograms recorded upon injections of RK at several different concentrations (Figure 2C). The two methods for calculating k_d were in good agreement. Furthermore, the equilibrium binding constant, K_d , calculated from the binding rates as the ratio of k_d/k_a agrees well with the steady-state K_d determination shown in Figure 1.

Myristoylation is required for recoverin to interact with membranes (14, 19, 26) and enhances recoverin's ability to inhibit rhodopsin phosphorylation by RK (7, 27). We used SPR to examine the influence of myristoylation on the direct binding between recoverin and RK. Figure 2 shows that the kinetics of RK binding to nonmyristoylated and myristoylated recoverin were slightly different. The on-rate of RK binding to nonmyristoylated recoverin was reproducibly faster than to the acylated form by 10–20%. Since the dissociation of RK from nonmyristoylated recoverin was also

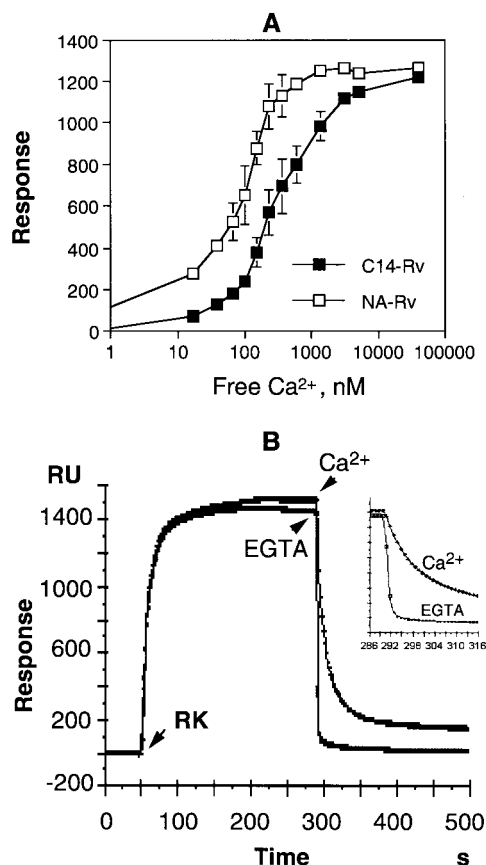


FIGURE 3: Effect of Ca^{2+} on RK–recoverin binding. (A) Solutions of RK (250 nM) at different free Ca^{2+} concentrations were injected across surfaces with equal densities of immobilized nonmyristoylated (NA-Rv) or myristoylated (C14-Rv) recoverin. The Ca^{2+} dependence is shown for the signal at equilibrium (100 s after the start of the RK injection). EGTA-buffered solutions of free Ca^{2+} from Molecular Probes (Eugene, Oregon) were used in this experiment. (B) Overlay plot of two identical injections of RK over recoverin at saturating Ca^{2+} . Immediately after the end of the sample flow, the solution was changed to 5 mM EGTA in buffer with no Ca^{2+} (squares) or the same running buffer with Ca^{2+} . The inset shows the dissociation phase of the same plot at higher resolution. In this experiment, the data points are taken at 2 Hz.

10–20% more rapid, the overall binding affinity of recoverin forms to RK was equal.

Previous studies demonstrated that Ca^{2+} is required for recoverin to inhibit RK, so we used SPR to determine the Ca^{2+} dependence of the bona fide protein–protein binding between recoverin and RK. Figure 3A shows that the $K_{0.5}$ for Ca^{2+} was 150 ± 50 nM for nonacylated (NA-Rv) and 400 ± 100 nM for myristoylated (C14-Rv) recoverin forms. The Ca^{2+} requirement was also confirmed by the effect of EGTA on the preformed recoverin–RK complex. Figure 3B shows that when RK is first bound to recoverin in the presence of $100 \mu\text{M}$ Ca^{2+} , subsequent injection of EGTA causes dissociation of RK in less than 1 s. This is in striking contrast to the slower dissociation rates detected at the end of an RK injection in the presence of Ca^{2+} . These results highlight the ability of SPR to measure rapid dissociation kinetics and demonstrate that dissociation of Ca^{2+} and the subsequent conformational changes in recoverin occur in less than 1 s.

RK uses ATP as a substrate both for rhodopsin phosphorylation and for autophosphorylation (11, 28). We used SPR to examine the effects of ATP and other nucleotides on the

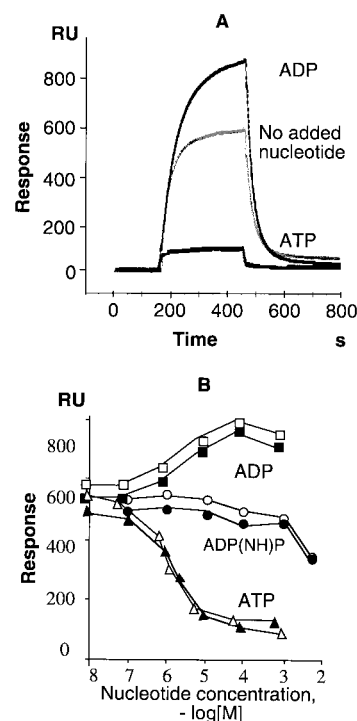


FIGURE 4: Influence of adenine nucleotides on binding of RK to recoverin. (A) Overlay plot of sensograms recorded when RK was injected across the recoverin-derivatized surface in the presence of $100 \mu\text{M}$ ATP and $100 \mu\text{M}$ ADP and in the absence of nucleotide. Prior to injection, RK was incubated with the nucleotide for 10 min at room temperature. (B) Dose dependence of the effect of the nucleotides. RK was injected across the surface at the indicated concentrations of ADP (squares), ADP(NH)P (circles), and ATP (triangles). Open symbols, NA-Rv; closed symbols, C14-Rv.

recoverin–RK interaction. Figure 4A shows that 0.1 mM ATP substantially inhibits the Rv–RK interaction whereas 0.1 mM ADP enhances it. Both ATP and ADP are effective at micromolar concentrations (Figure 4B) whereas 1 mM GTP, GDP, CTP, and XTP were ineffective. The nonhydrolyzable ATP analogue ADP(NH)P slightly inhibited the interaction but only at millimolar concentrations, suggesting that the effect may be due to a contaminant such as ATP. At 250 nM RK concentration, about $10\times$ more kinase bound to recoverin in the presence of ADP than in ATP. In the presence of ATP, the interaction was characterized by approximately 3 times slower association and 2 times faster dissociation rates (data not shown). The different binding kinetics indicate that low binding of RK in the presence of ATP was not due to residual “free” RK (reduction of active RK concentration) but rather due to the specific characteristic of ATP-treated RK.

The inhibitory effect of ATP could be caused either by autophosphorylation of RK or by an allosteric change induced in RK by ATP binding. To investigate the role of autophosphorylation, we measured RK binding in the presence or absence of protein phosphatase 2A (PP2A), an enzyme that dephosphorylates RK (11). Figure 5 shows that the ATP effect was nearly completely reversed by PP2A. The inset to Figure 5 confirms dephosphorylation of RK by PP2A and shows that the PP2A activity we used in this experiment was sufficient to completely dephosphorylate RK even in the presence of ATP. Noteworthy, the use of two other protein phosphatases, protein phosphatase λ (Calbiochem) and recombinant rabbit muscle protein phosphatase

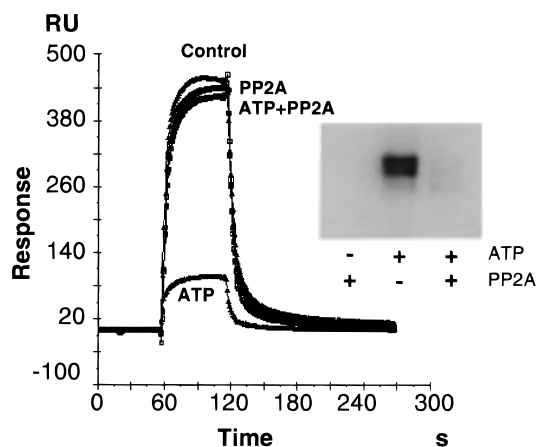


FIGURE 5: Autophosphorylation of RK is responsible for the inhibitory effect of ATP. RK was incubated with or without [32 P]-ATP in the presence or absence of PP2A as described under Materials and Methods. Aliquots of the same samples were injected across the recoverin chip or analyzed on SDS-PAGE followed by radioautography (inset). The band corresponds to RK.

1 α , PP1 (38), resulted in only a partial dephosphorylation of RK, and, accordingly, incomplete restoration of RK–recoverin binding (not shown).

The effects of ATP and ADP on recoverin–RK binding appear to represent two separate mechanisms. Since ADP enhances RK–recoverin binding, we examined its effect on the behavior of autophosphorylated RK. We first incubated RK with ATP to allow autophosphorylation, and then measured the binding of the autophosphorylated RK to recoverin in the presence or absence of ADP. We found that after autophosphorylation, ADP does not affect the autophosphorylation state of RK and that it does not enhance the binding of autophosphorylated RK to recoverin (data not shown). These results show that ADP stimulates the binding of recoverin only to RK that has not undergone autophosphorylation.

DISCUSSION

Recoverin binds to RK and inhibits its ability to phosphorylate photoactivated rhodopsin *in vitro*. We used SPR to demonstrate that the recoverin–RK interaction occurs with on- and off-kinetics which are significantly faster than in other interactions that have been analyzed by SPR such as G $\beta\gamma$ -phosducin (29), PDE γ -T α (30), and G α -G $\beta\gamma$ (Slepak and Satpaev, unpublished). The rapid kinetics may reflect a need to respond quickly to rapid changes in free Ca $^{2+}$ levels that occur within a photoreceptor cell (25, 31, 32).

We have also found that RK binds to immobilized calmodulin in a Ca $^{2+}$ -dependent manner (data not shown). The $K_{0.5}$ for Ca $^{2+}$ of this interaction was 3–5 μ M, which is beyond the physiologic range of free calcium in photoreceptors. Furthermore, calmodulin is a very poor inhibitor of RK: even when present at 10 μ M, calmodulin reduced RK activity by only 10–20% (33–35). This suggests that although both recoverin and calmodulin can bind to RK *in vitro*, only recoverin binding includes an additional interaction that specifically down-regulates rhodopsin phosphorylation by RK. In contrast, calmodulin effectively inhibits other GRKs (33–35), and it stimulates autophosphorylation of GRK5 (33). We have not, however, detected any obvious effects of calmodulin or recoverin on the extent of RK autophosphorylation in our experiments.

Our SPR analysis showed that the N-terminal myristoyl residue has little influence on association or dissociation rates of recoverin–RK complex formation. This is consistent with the observation that myristoylation is not needed for immobilized recoverin to bind RK (7). The insensitivity of the recoverin–RK interaction to N-myristoylation is still somewhat surprising because myristoylation does influence other activities of recoverin. N-Myristoylation is required for Ca $^{2+}$ -dependent binding of recoverin to membranes (14, 15, 19) and enhances its ability to inhibit RK (7, 22, 27) perhaps by increasing the local concentration of the Ca $^{2+}$ -bound recoverin on the membranes.

N-Myristoylation does affect the Ca $^{2+}$ dependence of the recoverin–RK interaction. We found $K_{0.5}$'s for Ca $^{2+}$ of 0.15 and 0.4 μ M for the nonacylated and myristoylated forms, respectively. Myristoylation may raise the free energy of the “R” state of recoverin, a conformation that favors Ca $^{2+}$ binding (36). In this state, the N-terminus is exposed, and the attached hydrophobic myristoyl residue is forced to be solvated. The effect of myristoylation on the affinity of recoverin for Ca $^{2+}$ has been previously measured in the absence of RK or membranes. Ames et al. directly measured Ca $^{2+}$ binding to pure recoverin and found K_d 's of 0.11 and 6.9 μ M to nonmyristoylated and 17 μ M to myristoylated protein (36). These values differ significantly from the ones we found for the direct recoverin–RK binding. The interaction of myristoylated recoverin with RK as determined by SPR occurs at 0.4 μ M Ca $^{2+}$, well below the K_d for Ca $^{2+}$ binding to pure myristoylated recoverin (17 μ M). This suggests that interaction of recoverin with RK stabilizes the “R” form of recoverin. Alternatively, the covalent linkage to the SPR chip may influence the free energy of either the “R” or the “T” form of recoverin, in a way mimicking the effect of the phospholipid membrane. The Ca $^{2+}$ dependencies of recoverin–RK interactions determined by SPR are also different from those of recoverin-mediated inhibition of RK activity (6, 7, 18). This difference may reflect the effect of membranes and/or a weaker interaction between recoverin and the autophosphorylated form of RK that should rapidly form in the presence of ATP added to the phosphorylation assay.

Since ATP interacts with RK as a substrate, we used SPR to examine the effects of adenine nucleotides on the recoverin–RK interaction. Surprisingly, we found that ATP strongly inhibits the interaction and ADP enhances it. The SPR analysis shown in Figure 4 revealed that the amount of RK bound to immobilized recoverin in ADP is approximately 10 \times that bound in ATP. This type of difference was not detected in previous studies analyzing rhodopsin phosphorylation. In those experiments, ATP (0.5 mM in a typical assay) was always present since it was needed as a substrate for RK.

Our results provide evidence for two separate effects of adenine nucleotides on the recoverin–RK interaction. Since nucleotides do not interfere with the SPR signal and are not known to interact with recoverin, we conclude that ATP and ADP affect RK. These effects appear to be the consequences of autophosphorylation of RK and ADP binding to RK. We attribute the ATP-mediated inhibition of recoverin–RK binding to RK autophosphorylation because protein phosphatase PP2A, which dephosphorylates RK, reverses the effect. Moreover, the nonhydrolyzable ATP analogue ADP-

(NH)P was significantly less effective than ATP. We also found that ADP enhances the interaction of recoverin specifically with unphosphorylated RK. The stimulatory effect of ADP may be simply explained by an ADP-induced conformation of RK that has a higher affinity to recoverin. The intracellular concentrations of ATP and ADP are 3 orders of magnitude higher than the micromolar $K_{1/2}$ of the effect of adenine nucleotides reported here. Therefore, RK should always be "charged" with either ADP or ATP in vivo, so the cycle of nucleotide binding and hydrolysis may regulate the RK—recoverin interaction.

The ability of ADP to enhance recoverin—RK binding may be responsible for an intriguing effect that recoverin has on the time course of rhodopsin phosphorylation (7, 8). The initial rate of rhodopsin phosphorylation by RK is unaffected by the presence of recoverin and Ca^{2+} . However, when recoverin— Ca^{2+} is present, the phosphorylation process is quickly terminated. It is possible that ADP formed during the initial transfer of γ -phosphate to rhodopsin may remain bound to RK, enhance recoverin binding, and stop further phosphorylation activity by RK. In principle, such a mechanism could have the effect of reducing photoreceptor dark-noise by acting somewhat like a coincidence detector. RK would initially be very active, even in the dark (i.e., high Ca^{2+}), and would rapidly quench isolated single activated rhodopsins. But ADP that remains bound following that first round of phosphorylation would then cause recoverin to bind and inhibit RK, thereby increasing the sensitivity of the cell to a second stimulus.

It is puzzling that recoverin can inhibit RK in vitro because RK undergoes rapid autophosphorylation which would be expected to dramatically reduce their interaction. A possible explanation for this might be that interaction of recoverin with autophosphorylated RK may be enhanced by the presence of membranes. Our observation that myristoylation does not affect the direct interaction of recoverin and RK, whereas it does enhance the ability of recoverin to inhibit RK in the presence of membranes (7, 27, 37), indirectly supports this idea. The concentration of both RK and recoverin in the outer segments is on the order of several micromoles. Since the binding affinity of phosphorylated RK to recoverin is about 6 μM , binding of recoverin to phosphorylated RK should still occur, albeit with less efficiency and a slower rate than with ADP-bound RK. Another factor that should be considered is the activity of protein phosphatase which may also regulate the extent of RK autophosphorylation in vivo. The effect of adenine nucleotides on the recoverin—RK interaction reported herein suggests a previously unappreciated complexity of RK regulation. Detailed understanding of the mechanism will require quantitative evaluation of the effects of lipids, rhodopsin, and recoverin on the binding of adenine nucleotides to RK as well as a study of the ATP and ADP effects on the recoverin—RK interaction at the membrane. Obtaining RK mutants deficient in binding lipid, rhodopsin, and recoverin as well as autophosphorylation and binding of the nucleotides would be extremely helpful in further dissecting of RK's functional cycle.

ACKNOWLEDGMENT

We thank Dr. E. Lee (University of Miami) for providing protein phosphatase PP1.

REFERENCES

1. Palczewski, K., and Benovic, J. L. (1991) *Trends Biochem. Sci.* 16, 387–391.
2. Kawamura, S., Hisatomi, O., Kayada, S., Tokunaga, F., and Kuo, C. H. (1993) *J. Biol. Chem.* 268, 14579–14582.
3. Dizhoor, A. M., Lowe, D. G., Olshevskaya, E. V., Laura, R. P., and Hurley, J. B. (1994) *Neuron* 12, 1345–1352.
4. Gorodovikova, E. N., Gimelbrant, A. A., Senin, I. I., and Philippov, P. P. (1994) *FEBS Lett.* 349, 187–190.
5. Sanada, K., Shimizu, F., Kameyama, K., Haga, K., Haga, T., and Fukada, Y. (1996) *FEBS Lett.* 384, 227–230.
6. Klenchin, V. A., Calvert, P. D., and Bownds, M. D. (1995) *J. Biol. Chem.* 270, 16147–16152.
7. Chen, C. K., Inglese, J., Lefkowitz, R. J., and Hurley, J. B. (1995) *J. Biol. Chem.* 270, 18060–18066.
8. Senin, I. I., Dean, K. R., Zargarov, A. A., Akhtar, M., and Philippov, P. P. (1997) *Biochem. J.* 321, 551–555.
9. Premont, R. T., Inglese, J., and Lefkowitz, R. J. (1995) *FASEB J.* 9, 175–182.
10. Pulvermüller, A., Palczewski, K., and Hofmann, K. P. (1993) *Biochemistry* 32, 14082–14088.
11. Buczylo, J., Gutmann, C., and Palczewski, K. (1991) *Proc. Natl. Acad. Sci. U.S.A.* 88, 2568–2572.
12. Palczewski, K., Ohguro, H., Premont, R. T., and Inglese, J. (1995) *J. Biol. Chem.* 270, 15294–15298.
13. Dizhoor, A. M., Ericsson, L. H., Johnson, R. S., Kumar, S., Olshevskaya, E., Zozulya, S., Neubert, T. A., Stryer, L., Hurley, J. B., and Walsh, K. A. (1992) *J. Biol. Chem.* 267, 16033–16036.
14. Dizhoor, A. M., Chen, C.-K., Olshevskaya, E., Sinelnikova, V. V., Philippov, P., and Hurley, J. B. (1993) *Science* 259, 829–832.
15. Zozulya, S., and Stryer, L. (1992) *Proc. Natl. Acad. Sci. U.S.A.* 89, 11569–11573.
16. Hughes, R. E., Brzovic, P. S., Klevit, R. E., and Hurley, J. B. (1995) *Biochemistry* 34, 11410–11416.
17. Tanaka, T., Ames, J. B., Harvey, T. S., Stryer, L., and Ikura, M. (1995) *Nature* 376, 444–447.
18. Ames, J. B., Tanaka, T., Ikura, M., and Stryer, L. (1995) *J. Biol. Chem.* 270, 30909–30913.
19. Lange, C., and Koch, K.-W. (1997) *Biochemistry* 36, 12019–12026.
20. Ray, S., Zozulya, S., Niemi, G. A., Flaherty, K. M., Brolley, D., Dizhoor, A. M., McKay, D. B., Hurley, J., and Stryer, L. (1992) *Proc. Natl. Acad. Sci. U.S.A.* 89, 5705–5709.
21. Zargarov, A. A., Senin, I. I., Alekseev, A. M., Shul'ga-Morskoi, S. V., Philippov, P. P., and Lipkin, V. M. (1997) *Bioorg. Khim.* 22, 483–488.
22. Sanada, K., Kokame, K., Yoshizawa, T., Takao, T., Shimonishi, Y., and Fukada, Y. (1995) *J. Biol. Chem.* 270, 15459–15462.
23. Gorodovikova, E. N., and Philippov, P. P. (1993) *FEBS Lett.* 335, 277–279.
24. Malmqvist, M. (1993) *Nature* 361, 186–187.
25. Ratto, G. M., Payne, R., Owen, W. G., and Tsien, R. Y. (1988) *J. Neurosci.* 8, 3240–3246.
26. Zozulya, S., and Stryer, L. (1992) *Proc. Natl. Acad. Sci. U.S.A.* 89, 11569–11573.
27. Calvert, P. D., Klenchin, V. A., and Bownds, M. D. (1995) *J. Biol. Chem.* 270, 24127–24129.
28. Lee, R. H., Brown, B. M., and Lolley, R. N. (1982) *Biochemistry* 21, 3303–3307.
29. Xu, J., Wu, D., Slepak, V. Z., and Simon, M. I. (1995) *Proc. Natl. Acad. Sci. U.S.A.* 92, 2086–2090.
30. Slepak, V. Z., Artemyev, N. O., Zhu, Y., Dumke, C. L., Sabacan, L., Sondek, J., Hamm, H. E., Bownds, M. D., and Arshavsky, V. Y. (1995) *J. Biol. Chem.* 270, 14319–14324.
31. Younger, J. P., McCarthy, S. T., and Owen, W. G. (1996) *J. Neurophysiol.* 75, 354–366.
32. Gray-Keller, M. P., and Detwiler, P. B. (1994) *Invest. Ophthalmol. Visual Sci.* 35, 1486.
33. Pronin, A. N., Satpaev, D. K., Slepak, V. Z., and Benovic, J. L. (1997) *J. Biol. Chem.* 272, 18273–18280.

34. Chuang, T. T., Paolucci, L., and De Blasi, A. (1996) *J. Biol. Chem.* 271, 28691–28696.
35. Haga, K., Tsuga, H., and Haga, T. (1997) *Biochemistry* 36, 1315–1321.
36. Ames, J. B., Porumb, T., Tanaka, T., Ikura, M., and Stryer, L. (1995) *J. Biol. Chem.* 270, 4526–4533.
37. Senin, I. I., Zargarov, A. A., Alekseev, A. M., Gorodovikova, E. N., Lipkin, V. M., and Philippov, P. P. (1995) *FEBS Lett.* 376, 87–90.
38. Zhang, L., and Lee, E. Y. (1997) *Biochemistry* 36, 8209–8214.
BI9804986